N, 7.4.

E. Ligand 2. Triethylamine (2.0 mL, 0.0143 mol) was added to a stirred solution of **11**·3HCl (1.3 g, 0.0047 mol) in water (10 mL) under N_2, and after 5 min **16** (6.3 g, 0.0145 mol) in THF (80 mL) was added all at once. There was an immediate formation of a bright yellow two-phase mixture. After 1 h the cloudy mixture was partially cleared by the addition of water (2 mL) and THF (20 mL), and after an additional 5 h more Et_3N (2.0 mL, 0.0143 mol) was added. The mixture was stirred for a total of 20 h, and then the THF was removed under reduced pressure. The residue was extracted with ethyl acetate (2 × 75 mL), and the combined organic layers were washed with water (5 × 120 mL) and brine (4 × 100 mL) and were dried over Na_2SO_4. After the extract was passed through a short column of Florisil, ethyl acetate was removed under reduced pressure, yielding **16** (6.0 g) as a light green foam. This was then dissolved in methanolic ammonia (65 g, 8%, w/w) and the mixture was allowed to stand at room temperature for 1.5 h. The bright yellow, slightly cloudy solution was filtered through Celite, and the solvent was removed under reduced pressure, yielding a bright yellow oil, which was taken up in hot EtOH (25 mL). Upon standing (10 h at room temperature, 2 days at 4 °C, and 1 day at −20 °C), a yellow solid was deposited, which was recrystallized twice from hot EtOH, yielding **2** (1.76 g, 50%; mp 162–165 °C) as an off-white solid. ^{1}H NMR Me_2SO-d_6): δ 2.4–2.8 (m, 6 H), 3.7–4.1 (m, 6 H), 4.2 (d, J = 5 Hz, 6 H), 7.0 (s, 3 H), 7.2–7.7 (m, 15 H), 8.4 (br t, J = 5 Hz, 3 H), 9.8 (br s, 3 H). Anal. Calcd for $C_{39}H_{42}N_6O_9$: C, 63.4; H, 5.7; N, 11.4. Found: C, 63.2; H, 5.8; N, 11.3.

F. Iron(III) Complexes. A solution of $Fe(NH_4)(SO_4)_2$·$12H_2O$ (0.015 57 g, 3.23 × 10^{-5} mol) in water (2 mL) was treated with **1** (0.018 57 g, 3.23 × 10^{-5} mol) in MeOH (2 mL). The purple milky solution was made up to 100 mL with a pH 8.50 borax buffer, producing a clear violet solution that displayed absorptions (Varian 2300 spectrophotometer) at λ_{max} = 498 nm (ϵ = 4697 M^{-1} cm^{-1}) and λ_{max} = 328 nm (ϵ = 17 900 M^{-1} cm^{-1}). The spectrum showed no change over several weeks.

A solution of $Fe(NH_4)(SO_4)_2$·$12H_2O$ (0.012 05 g, 2.50 × 10^{-5} mol) in water (2 mL) was treated with **2** (0.018 47 g, 2.50 × 10^{-5} mol) in DMF (10 mL), producing a clear red solution. DMF (65 mL) and a pH 8.50 borax buffer (22 mL) were added to this solution in portions, with sufficient DMF being added before the buffer to prevent the appearance of a fluffy orange-red precipitate. The total volume was made up to 100 mL with the buffer, producing an orange-red solution that exhibited only a broad absorption at λ_{max} = 428 nm (ϵ = 3466 M^{-1} cm^{-1}). The absorption reached its maximum intensity after ~20 h and remained unchanged for at least 5 days.

Stability Constants. For the determination of the stability constant of the iron complex, the same procedure was followed except that Na_2EDTA·$2H_2O$ (1 or 2 equiv based on **2**) dissolved in a little of the buffer was added after iron and the ligand **2** had been mixed. DMF and the rest of the buffer were then added as before. The absorption spectra showed that the intensity of the absorption at 428 nm in the case of 1 equiv of added Na_2EDTA·$2H_2O$ reached a maximum value after 5 h, a showing 23.8% loss of intensity. For the 2 equiv of added Na_2EDTA·$2H_2O$ the maximum value was reached in under 5 h, showing a 35.0% loss of intensity. Both of these solutions deposited a precipitate on standing after ~36 h.

Instrumentation. The ^{1}H NMR spectra were obtained on a Varian T-60 spectrometer, and the UV spectra were run on a Varian 2300 spectrophotometer.

Acknowledgment. This work was supported by grants from the Natural Sciences and Engineering Council of Canada, the Atkinson Foundation, and the J. P. Bickell Foundation.

Contribution from the Department of Chemistry, Princeton University, Princeton, New Jersey 08544

Ultraviolet Resonance Raman Study of Deoxyguanosine Monophosphate and Its Complexes with *cis*-$(NH_3)Pt^{2+}$, Ni^{2+}, and H^+

Joseph R. Perno, Dory Cwikel, and Thomas G. Spiro*

Received May 23, 1986

Raman spectra are reported with deep ultraviolet excitation at 240 and 218 nm for dilute (5 mM) aqueous solutions of 2′-deoxyriboguanosine 5′-monophosphate (dGMP), its N7-protonated form (pH 1.5), its 1:1 complex with aqueous Ni^{2+}, and its 1:1 and 2:1 complexes with *cis*-$(NH_3)_2Pt^{2+}$. The C=O6 stretching band at 1677 cm^{-1} in dGMP shifts up to 1702 cm^{-1} on N7 protonation and to 1686 cm^{-1} in the 2:1 Pt complex, reflecting the polarizing effect of these positive centers. In the Ni complex, however, this band shifts down to 1660 cm^{-1}, an effect attributed to intramolecular H bonding of the carbonyl oxygen atom by Ni-bound H_2O, as observed in the crystal structure. In the 1:1 Pt complex, a smaller downshift is seen, to 1670 cm^{-1}, and is suggested to be the resultant of opposing effects of polarization and intramolecular H bonding via the Pt-bound H_2O molecule; this H_2O is displaced by another guanine N7 in the 2:1 complex. Several guanine ring modes show progressive increases or decreases in frequency and/or intensity upon binding Ni, Pt, and H^+ due to polarization. Guanine modes at 682 and 855 cm^{-1} in dGMP, which are known to be sensitive to the sugar conformation, develop prominent shoulders at 666 and 864 cm^{-1} in the Ni and Pt complexes, and also in riboguanosine 5′-monophosphate (rGMP). These additional components are attributed to molecules with a C3′-endo ribose configuration, while the 682- and 855-cm^{-1} bands are associated with the C2′-endo conformation, which is dominant in dGMP. The crystal structure of the Ni complex shows a C3′-endo conformation, which allows the 5′-monophosphate linkage to accept H bonds from Ni^{2+}-bound H_2O molecules. It is suggested that this structural feature is only partially retained in solution. Prominent 666-cm^{-1} C3′-endo bands are also seen for Pt (but not Ni) complexes of 3′-dGMP and 2′-deoxyguanosine. Pt binding is suggested to stabilize the C3′-endo conformation via an electronic polarization effect.

Introduction

It has recently become possible to obtain Raman spectra with deep ultraviolet excitation by using pulsed YAG lasers and various frequency shifting devices.[1-4] This technology has made it possible to explore resonance effects in Raman spectra of simple aromatic chromophores, including aromatic side chains of proteins[5-12] and the purine and pyrimidine bases of nucleic acids.[13-16] Rich spectra of purine and pyrimidine ring modes have been reported, with the enhancement pattern varying strongly with laser excitation wavelength, as different π–π^* excited states are accessed. Variable-wavelength excitation can therefore be used to sort out and identify the different vibrational modes, whose overlap tends to obscure the band assignments in nonresonance Raman spectra

* To whom correspondence should be addressed.

(1) Ziegler, L. D.; Hudson, B. S. *J. Chem. Phys.* **1981**, *74*, 982.
(2) Ziegler, L. D.; Hudson, B. S. *J. Chem. Phys.* **1983**, *79*, 1134.
(3) Asher, S. A.; Johnson, C. R.; Murtaugh, J. *Rev. Sci. Instrum.* **1983**, *54*, 1657.
(4) Fodor, S. P. A.; Rava, R. P.; Copeland, R. A.; Spiro, T. G. *J. Raman Spectrosc.*, in press.
(5) Rava, R. P.; Spiro, T. G. *J. Am. Chem. Soc.* **1984**, *106*, 4062–4064.
(6) Johnson, C. R.; Ludwig, M.; O'Donnell, S.; Asher, S. A. *J. Am. Chem. Soc.* **1984**, *106*, 5008–5010.
(7) Rava, R. P.; Spiro, T. G. *J. Phys. Chem.* **1985**, *89*, 1856–1861.
(8) Rava, R. P.; Spiro, T. G. *Biochemistry* **1985**, *24*, 1861–1865.
(9) Copeland, R. A.; Dasgupta, S.; Spiro, T. G. *J. Am. Chem. Soc.* **1985**, *107*, 3370–3371.

0020-1669/87/1326-0400$01.50/0

with visible wavelength excitation. Moreover, the sensitivity of ultraviolet resonance Raman (UVRR) spectroscopy is high, and dilute samples (0.1–10 mM) are conveniently studied.

In this study we explore the utility of UVRR spectroscopy in studying the structural consequences of metal and proton binding to the guanine N7 position in 2′-deoxyriboguanosine 5′-monophosphate, dGMP. Metal binding to nucleic acids is a subject of general biological interest,[17-19] and the binding of *cis*-dichlorodiammineplatinum(II), (*cis*-DDP) has attracted much attention because of the effectiveness of *cis*-DDP in cancer chemotherapy.[20-22] It is known that *cis*-DDP hydrolyzes in neutral aqueous solution to *cis*-$(NH_3)_2Pt(OH)H_2O^+$ (as well as other hydrolysis products), which interacts with DNA regions that are rich in guanine (G) and cytidine (C). The predominant mode of binding is believed to involve chelation by N7 atoms of adjacent G residues on a given strand, and the structure of a model complex with d(pGpG) has recently been determined by X-ray crystallography[23] and NMR.[24] The possible effects on DNA conformation of *cis*-$(NH_3)_2Pt^{2+}$ binding to adjacent G's has been explored with molecular mechanics calculations.[25]

The mode of interaction of *cis*-$(NH_3)_2Pt^{2+}$ with a single guanine residue has not, however, been completely clarified. Although N7 is almost certainly the primary site for coordination,[26,27a] initial proposals for a N7–O6 chelate structure[27b,c] have not been supported by subsequent evidence,[28] and steric arguments have been advanced against such a structure,[29,48] although it may be stabilized when the keto form of G is converted to the enolate form by N1 deprotonation.[30] The crystal structures of the aquated Ni^{2+} complexes of IMP[31a] and dGMP[31b] show that N7 coordination can be augmented by intramolecular H bonding of metal-bound H_2O to the carbonyl O6 atom, and also to the 5′-monophosphate group. The phosphate interaction changes the conformation of the ribose ring to C3′-endo from C2′-endo, the conformation favored in uncomplexed dGMP. H-bonding to C=O6 has also been proposed[27a,32a] for *cis*-$(NH_3)_2Pt^{2+}$ bound to G residues but has not definitely been established crystallographically. Infrared spectra have been reported for solid metal–dGMP complexes including Ni–dGMP.[32b]

In the present study we find clear evidence for intramolecular H-bonding to the C=O6 group, via a downshift in its stretching frequency for 1:1 complexes with aquated Ni^{2+} and *cis*-$(NH_3)_2Pt^{2+}$; in contrast the 2:1 *cis*-$(NH_3)_2Pt^{2+}$ complex, in which the Pt-bound H_2O is displaced by a second G, shows an upshift in the C=O6 frequency, due to polarization, as does N7-

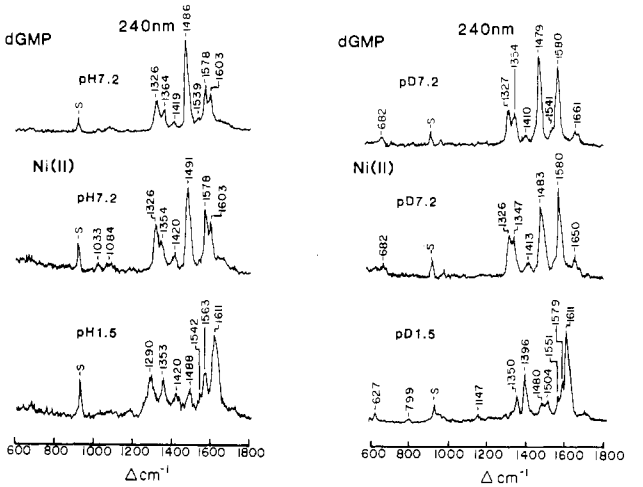

Figure 1. UVRR spectra, obtained with 240-nm excitation, for aqueous dGMP at pH 7.2 (top) and 1.5 (N7-protonated form, bottom) and the 1:1 complex with Ni^{2+} (middle), in H_2O (left) and D_2O (right). The band marked S is due to ClO_4^-, present as an internal standard.

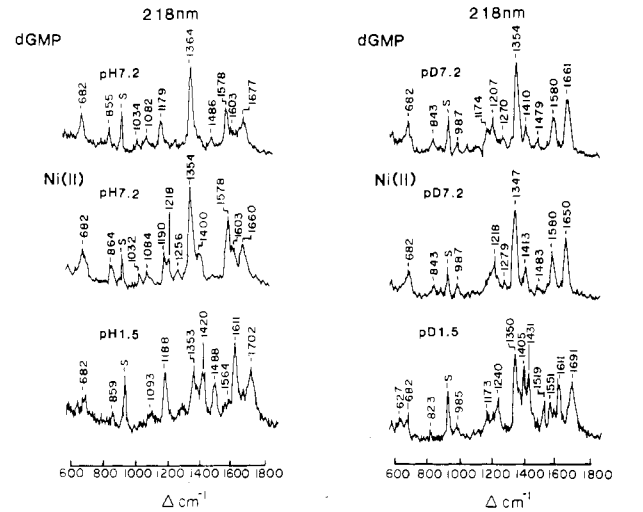

Figure 2. As Figure 1, but with 218-nm excitation.

(10) Copeland, R. A.; Spiro, T. G. *Biochemistry* **1985**, *24*, 4960–4968.
(11) Mayne, L. C.; Ziegler, L. D.; Hudson, B. *J. Phys. Chem.* **1985**, *89*, 3395–3398.
(12) Dudik, J. M.; Johnson, C. R.; Asher, S. A. *J. Phys. Chem.* **1985**, *89*, 3805–3814.
(13) Ziegler, L. D.; Hudson, B.; Strommen, D. P.; Peticolas, W. L. *Biopolymers* **1984**, *23*, 2067–2081.
(14) Fodor, S. P. A.; Rava, R. P.; Hays, T. R.; Spiro, T. G. *J. Am. Chem. Soc.* **1985**, *107*, 1520–1529.
(15) Kubasek, W. L.; Hudson, B.; Peticolas, W. L. *Proc. Natl. Acad. Sci. U.S.A.* **1985**, *82*, 2369–2373.
(16) Fodor, S. P. A.; Spiro, T. G. *J. Am. Chem. Soc.* **1986**, *108*, 3198–3205.
(17) Marzilli, L. G. *Prog. Inorg. Chem.* **1977**, *23*, 255.
(18) *Nucleic Acid-Metal Ion Intraction*; Spiro, T. G., Ed.; Wiley-Interscience: New York, 1980.
(19) (a) Behe, M.; Felsenfeld, G. *Proc. Natl. Acad. Sci. U.S.A.* **1981**, *78*, 1619–1623. (b) Behe, M.; Zimmerman, S.; Felsenfeld, G. *Nature (London)* **1981**, *293*, 233.
(20) Rosenberg, B. *Biochimie* **1978**, *60*, 859.
(21) (a) Lippard, S. J., Ed. *Platinum, Gold, and Other Metal Chemotherapeutic Agents*; ACS Symposium Series 209; American Chemical Society: Washington, DC, 1983. (b) Pinto, A. L.; Lippard, S. J. *Biochim. Biophys. Acta* **1985**, *780*, 167.
(22) (a) Marcelis, A. T. M.; Reedijk, J. *Recl.: J. R. Neth. Chem. Soc.* **1983**, *102*, 121. (b) Reedijk, J.; den Hartog, J. H. J.; Fichtinger-Schepman, A. M.; Marcelis, A. T. M. *Platinum Coordination Complexes in Cancer Chemotherapy*; Martinus Nijhoff: Boston, MA, 1983 p 39. (c) Marcelis, A. T. M.; van Kralingen, C. G.; Reedijk, J. *J. Inorg. Biochem.* **1980**, *13*, 213. (d) Marcelis, A. T. M.; Erkelens, C.; Reedijk, J. *Inorg. Chim. Acta* **1984**, *91*, 129.
(23) Sherman, S. E.; Gibson, D.; Wang, A. H.-J.; Lippard, S. J. *Science (Washington, D.C.)* **1985**, *230*, 412.
(24) (a) Girault, J. P.; Chottard, G.; Lallemand, Y.-Y.; Chottard, J.-C. *Biochemistry* **1982**, *21*, 1352. (b) Hartog, J. H. J.; Altona, C.; Chottard, J. C.; Girault, J. P.; Lallemand, J. Y.; deLeeuw, F. A. A. M.; Marcelis, A. T. M.; Reedijk, J. *Nucleic Acids Res.* **1982**, *10*, 4715–4730.
(25) (a) Kozelka, J.; Petsko, G. A.; Quigley, G. J.; Lippard, S. J. *J. Am. Chem. Soc.* **1985**, *107*, 4079–4081. (b) Kozelka, J.; Petsko, G. A.; Quigley, G. J.; Lippard, S. J. *Inorg. Chem.* **1986**, *25*, 1075–1077.
(26) Chu, G. Y. H.; Mansy, S.; Duncan, R. E.; Tobias, R. S. J. *J. Am. Chem. Soc.* **1978**, *100*, 593.
(27) (a) Kong, P. C.; Theophanides, T. *Inorg. Chem.* **1974**, *13*, 1167. (b) Goodgame, D. M. L.; Jeeves, I.; Phillips, F. L.; Shapski, A. C. *Biochim. Biophys. Acta* **1975**, *378*, 153. (c) Macquet, J. P.; Theophanides, T. *Bioinorg. Chem.* **1975**, *5*, 59.
(28) Raudaschl-Sieber, G.; Marzilli, L. G.; Lippert, B.; Shinozuka, K. *Inorg. Chem.* **1985**, *24*, 989–990.
(29) Barton, J. K.; Lippard, S. J. In *Nucleic Acid-Metal Ion Interaction*; Spiro, T. G., Ed.; Wiley-Interscience, New York, 1980; p 31.
(30) Hadjiliadis, N.; Theophanides, T. *Inorg. Chim. Acta* **1976**, *16*, 77.
(31) (a) Clark, G. R.; Orbell, J. D. J. *J. Chem. Soc., Chem. Commun.* **1974**, 139. (b) Gellert, R. W.; Shiba, K. J.; Bau, R. *Biochim. Biophys. Res. Commun.* **1979**, *88*, 1449.
(32) (a) Wing, R. M.; Pjura, P.; Drew, H. R.; Dickerson, R. E. In *Structure and Biological Activity*, Griffin, J. F., Duax, W. L., Eds.; Elsevier: Amsterdam, 1982; p 337. (b) Theophanides, T.; Tajmir-Riakki, H. A. *Structure and Motion: Membranes, Nucleic Acids and Proteins*; Clementi, E., Corongia, G., Sarma, M. H., Sarma, R. H., Eds.; Adenine: Guilderland, NY, 1985; p 521. *Spectroscopy of Biological Molecules*; Sandorfy, C., Theophanides, T., Eds.; D. Reidel: Dordrecht, The Netherlands, 1983; p 137.

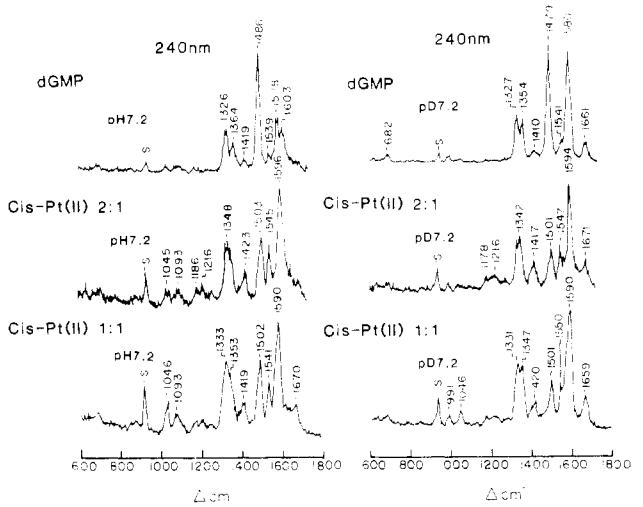

Figure 3. UVRR spectra, with 240-nm excitation, for aqueous dGMP (top) and its 2:1 (middle) and 1:1 (bottom) complexes with *cis*-$(NH_3)_2Pt^{2+}$, prepared as described in the Experimental Section, in H_2O (left) and D_2O (right). The band marked S is due to ClO_4^-.

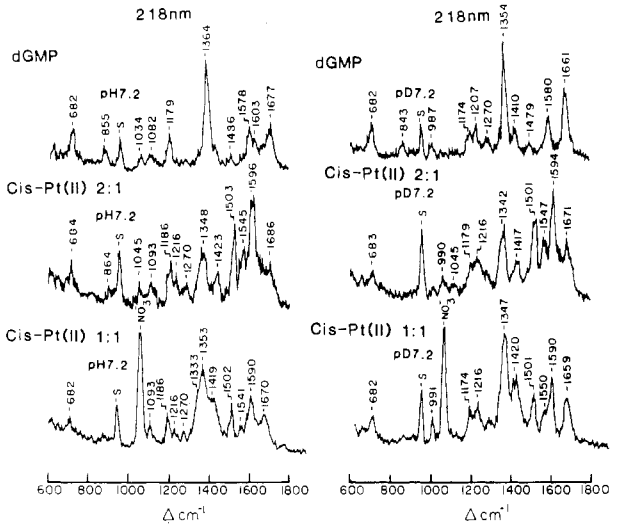

Figure 4. As Figure 3, but with 218-nm excitation. The peak labeled NO_3^- is due to the NO_3^- present in the *cis*-$(NH_3)_2Pt(H_2O)_2^{+}$ solution used in the preparation of the 1:1 complex; it is enhanced at 218 nm in resonance with a NO_3^- electronic transition (λ_{max} = 212 nm).

protonated GMP. Polarization effects are also seen in frequency and/or intensity changes for several guanine ring modes. The guanine modes that are conformational markers for the ribose ring show evidence for a mixture of C2′- and C3′-endo conformations in the Ni complex, suggesting that the intramolecular H-bonding to the 5′-monophosphate group is retained only partially in solution. Similar mixtures are seen for the *cis*-$(NH_3)_2Pt^{2+}$ complexes with dGMP. However, H-bonding to phosphate from Pt-bound NH_3 is not required to stabilize the C3′-endo conformation since an increase in the C3′-endo population is also seen when the *cis* Pt complex binds to 2′-deoxyguanosine 3′-monophosphate or even 2′-deoxyguanosine, which has no phosphate group. While *cis*-$(NH_3)_2Pt^{2+}$ binding to GMP has previously been studied extensively by nonresonance Raman spectroscopy,[26] the interpretation was complicated by band overlaps and by aggregation phenomena at the high concentrations required.

Experimental Section

Materials. The nucleotides (Na^+ salts of 5′-dGMP, 3′-dGMP, and deoxyguanosine) and silver nitrate were obtained from Sigma, nickel(II) chloride and sodium perchlorate were obtained from Fisher, and *cis*-DDP was obtained from Strem. All compounds were of the highest purity and used without further purification. Deionized water was purified through a Milli Q/uF Millipore system. Deuterium oxide was obtained from MSD Isotopes.

Preparation of the Complexes. Nickel(II) chloride was added to a stoichiometric amount of 5′-dGMP in water; pH/pD was monitored on a Corning Model 150 digital pH meter and was adjusted with NaOH for aqueous samples and NaOD for samples in D_2O. For D_2O samples the readings were corrected for the deuterium isotope effect.[33] In the case of the protonated species, concentrated HCl/DCl was used to adjust the pH.

Preparation of well-defined *cis*-$(NH_3)_2Pt$ adducts requires careful control of reaction conditions.[22c,34] The 2:1 complex [*cis*-Pt(5′-dGMP)$_2$$(NH_3)_2$] was formed by addition of a stoichiometric amount of solid *cis*-DDP to a 5 mM solution of 5′-dGMP in 10 mM phosphate buffer. The reaction was allowed to proceed at 37 °C overnight in the dark. For the preparation of the 1:1 complex, 5 mL of a 10 mM solution of aquated *cis*-DDP was added to 5 mL of a 10 mM solution of 5′-dGMP in 20 mM phosphate buffer. Sample purity (reaction conditions yielded 85–90% of the 1:1 and 100% of the 2:1 complex) and integrity were monitored before and after laser exciation by ^1H NMR spectroscopy (Bruker WM 250 MHz) as described in ref 22c. All solutions were 0.3 M in sodium perchlorate, which was added as an internal standard for the Raman experiments.

Method. Raman spectra were obtained with 218- and 240-nm excitation as described elsewhere.[4] The spectra were recorded with 0.05 Å/s increments and 8-cm^{-1} spectral resolution. Spectra of the 5′-dGMP solutions and Ni complexes are the sum of three–four scans whereas those of the cis Pt complex and protonated adducts are the sum of seven–nine consecutive scans.

Results

Figures 1–4 show UVRR spectra obtained with 240- and 218-nm excitation for dGMP at pH 7.2 and 1.5 (N7-protonated) and its 1:1 complex with aqueous Ni^{2+} and 1:1 and 2:1 complexes with *cis*-$(NH_3)_2Pt^{2+}$, formed and monitored as described in the Experimental Section. These two wavelengths were chosen to bring out the greatest number of guanine bands via the different enhancement patterns.[14] A total of 13 bands can be identified and tracked from one complex to another. Also shown in the figures are spectra in D_2O solution, obtained to aid in band identification. The exchange of the NH_2 amino, and especially the N1H imino protons for deuterons changes the normal mode composition somewhat and helps to clarify some of the bands.[14] In Table I the band frequencies are correlated among the different dGMP complexes, and are associated with guanine mode frequencies recently calculated via an ab initio normal coordinate analysis by Tsuboi and co-workers,[35] who have suggested the approximate mode descriptions given in Table I.[35b] For N7-protonated dGMP, the correlations are slightly less secure, because of the probable mixing in of the N7–H bending coordinate, and additional complications arise in the D_2O spectrum because of the additional H/D exchange at N7; indeed there seem to be several extra bands in this spectrum. Nevertheless, most of the bands do correlate straightforwardly with those of the other dGMP complexes.

Figure 5 is an expanded view of 218-nm-excited spectra in the 600–900-cm^{-1} region, where conformationally sensitive G modes are found, for dGMP and its 1:1 aquated Ni^{2+} complex, as well as for rGMP.

Discussion

The C=O6 Carbonyl Stretch. Figure 6 is a structural diagram of the 1:1 dGMP–Ni^{2+} complex as determined by X-ray crystallography;[31b] it also gives the numbering system for the guanine ring. The nickel ion is coordinated to N7 and to five water molecules, one of which is H bonded to the carbonyl O6 atom. The highest frequency band in the UVRR spectra is due primarily to C=O6 stretching;[35] it is more strongly enhanced with 218-nm excitation than with 240-nm excitation.[14] For dGMP itself, this band appears at 1677 cm^{-1} in H_2O and, more strongly, at 1661 cm^{-1} in D_2O. The downshift and intensification in D_2O probably

(33) Gasoe, P. K.; Long, F. A. *J. Phys. Chem.* **1960**, *64*, 188.
(34) Miller, S. K.; Marzilli, L. G. *Inorg. Chem.* **1985**, *24*, 2421.
(35) (a) Nishimura, Y.; Tsuboi, M.; Kato, S.; Morokuma, K. *Bull. Chem. Soc. Jpn.* **1985**, *58*, 638. (b) Tsuboi, M.; Nishimura, Y.; Hirakawa, A. Y.; Peticolas, W. L. In *Biological Applications of Raman Spectroscopy*; Spiro, T. G., Ed., Wiley: New York, 1986; Vol. 1.

Table I. UVRR Band Frequencies (cm^{-1}) for dGMP and Its Adducts, in H_2O and D_2O, Correlated with the Vibrational Modes of Guanine[35b]

guanine mode[a]			UVRR bands				
ν_{calcd}	designations[b]		dGMP	(dGMP)Ni	(dGMP)Pt	$(dGMP)_2Pt$	$dGMPH^+$
1751	$\nu_{C=O}$	H_2O	1677[c]	1660	1670	1686	1702
		D_2O	1661	1650	1659	1671	1691
1635	$NH_2(sc)$	H_2O	1603[d]	1603			
		D_2O					
1602	ν_a^6	H_2O	1578[c]	1578	1590	1596	1611
		D_2O	1580	1580	1590	1594	1611
1542	ν_b^6	H_2O	1539[d]		1541	1545	1563
		D_2O	1541		1550	1547	1551
1501	$Kk + \nu_1^5$	H_2O	1486[d]	1491	1502	1503	1488
		D_2O	1479	1483	1501	1501	1504
							1480
1444	$Kk - \nu_1^5$	H_2O	1419[d]	1420	1419	1423	1420
		D_2O	1410	1413	1420	1417	1431
							1405
1405	$\nu\delta_b^6$	H_2O	1363[c]	1354	1353	1348	1353
		D_2O	1354	1347	1347	1342	1350
1351	$\nu_2^5 + \delta_{N_9H}$	H_2O	1326[d]	1326	1333	1348	
		D_2O	1327	1326	1331	1342	
1179	Br^5	H_2O	1179[c]	1190	1186	1186	1188
		D_2O	1174	1218 (sh)	1174	1179	1173
813	$Tr + \delta_\perp^5$	H_2O	855[c]	864		863	859
		D_2O	843	843			823
684	$\delta_b^6 + \delta_\perp^5$	H_2O	682	682	682	684	682
		D_2O	682	682	682	683	682

[a] From ref 35b. [b] Symbols (see ref 35b for details): $\nu_{C=O}$, C=O6 stretching $NH_2(sc)$, amine NH_2 scissors mode; ν_i^6, six-membered ring modes derived from benzene 1595 cm^{-1} (e_{2g}; i = a, b) and 1484 cm^{-1} (e_{1u}; i = δ_a, δ_b) modes; Kk, derived from the benzene Kekulé mode, 1308 cm^{-1} (b_{2u}); δ_b^6, derived from the benzene 605-cm^{-1} (e_{2g}) mode; Tr, derived from the benzene triangle vibrations, 1010 cm^{-1} (b_{1u}). ν_i^5, five-membered ring stretching vibrations, systematic (i = 2) and antisymmetric (i = 1) with respect to the horizontal 2-fold axis. Br^5, five-membered ring breathing mode. $\delta_\perp^5$, five-membered ring deformation mode (moving the center of gravity perpendicular to the horizontal 2-fold axis). [c] Most clearly seen with 218-nm excitation. [d] Most clearly seen with 240-nm excitation.

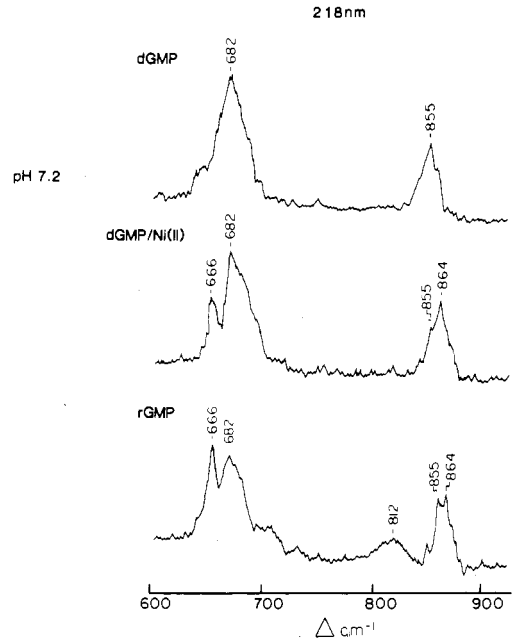

Figure 5. High-resolution scans of the 600–900-cm^{-1} region of the 218-nm-excited UVRR spectra of aqueous rGMP (bottom), dGMP (top), and the 1:1 Ni–dGMP complex (middle).

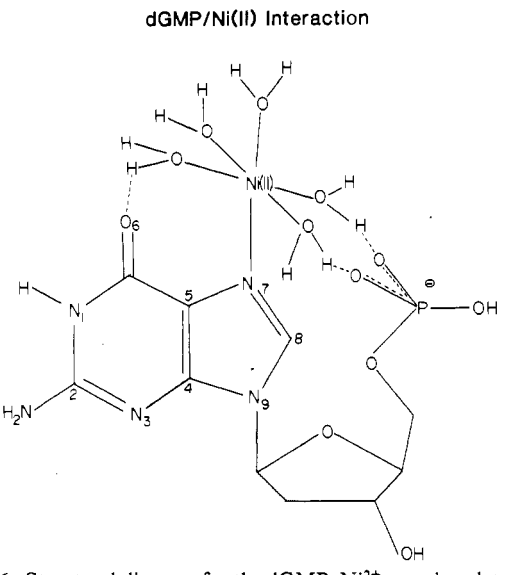

Figure 6. Structural diagram for the dGMP–Ni^{2+} complex, determined by X-ray crystallography.[31b]

reflect greater ring mode character for the band, due to a change in normal mode composition caused by the N1H/D exchange.

When N7 is protonated, the band shifts up to 1702 cm^{-1} in H_2O and 1691 cm^{-1} in D_2O (Figure 2). This upshift is attributable to a strengthening of the C=O6 bond due to the polarizing effect of the N7 proton on the entire guanine π system. Somewhat smaller upshifts, to 1686 and 1671 cm^{-1}, are seen in the 2:1 Pt complex (Figure 4); polarization by Pt(II) is somewhat less effective than by H^+, a conclusion also reached by Tobias and co-workers.[26] In the 1:1 Pt complex, however, the band shifts down by 7 cm^{-1} in H_2O, although by only 2 cm^{-1} in D_2O. A larger downshift is seen in the Ni complex, by 17 and 11 cm^{-1} in H_2O and D_2O, respectively. We attribute the downshifts to the effect of the intramolecular H bond, which weakens the C=O6 bond. The effect is greater in H_2O than in D_2O because of the more purely C=O stretching character in the former case. The downshift seen for the 1:1 Pt complex is a definite indication of intramolecular H bonding; it is smaller for Pt than for Ni because Pt is more polarizing and the polarization effect counters the H-bonding effect.

Other Ring Modes. Systematic changes of several guanine ring modes are associated with complexation. For example the 1578-cm^{-1} band of dGMP shifts up to 1590 and 1596 cm^{-1} in the 1:1 and 2:1 Pt complexes and to 1611 cm^{-1} upon N7-protonation; the relative intensity of the band also increases in the same order, with increasing polarization. Similarly the 1539-cm^{-1} band, which is quite weak for dGMP (see the 240-nm-excited spectrum, Figure 1), shifts up and intensifies in the same series. On the other hand

the 1486-cm^{-1} band, the strongest feature in the 240-nm-excited dGMP spectrum, weakens as it shifts up in frequency from the complex with Ni (1491 cm^{-1}), to 1:1 Pt (1502 cm^{-1}) and 2:1 Pt (1503 cm^{-1}); the weakening, but not the frequency upshifting, continues to the N7-protonated form (1488 cm^{-1}). A weakening of this band in nonresonant Raman spectra of nucleic acids has been associated with cationic interactions at guanine N7.[36] The 1364-cm^{-1} band, which is the strongest feature of the 218-nm-excited dGMP spectrum, weakens as it shifts down in frequency upon complexation from Ni (1354 cm^{-1}) to 1:1 Pt (1353 cm^{-1}) to 2:1 Pt (1348 cm^{-1}); the N7-protonated band is weaker but also slightly higher in frequency, 1353 cm^{-1}, than that for the 2:1 Pt complex.

These major bands are quite different from one another in character (see Table I). Thus the 1578- and 1539-cm^{-1} bands are associated with the six-membered ring, primarily, while the 1486- and 1363-cm^{-1} bands have considerable five-membered ring character (Table I). Thus it is evident that the electronic effects of cationic polarization at N7 are spread throughout the guanine ring structure.

Sugar-Conformation-Sensitive Guanine Modes. A mode at 682 cm^{-1} in dGMP[37-43] is known to be sensitive to the conformation of the ribose ring, presumably via vibrational coupling with unobserved ribose vibrational modes. The 682-cm^{-1} frequency is characteristic of the C2′-endo sugar conformation, seen in dGMP and in B-form DNA. The frequency shifts dramatically, to 625 cm^{-1}, in Z-form DNA, due to a change to C3′-endo sugar conformation and also a *syn* orientation of the glycosidic bond in this left-handed helical structure. In A-form DNA, the glycosidic orientation remains *anti*, as it is in B-form DNA, but the sugar conformation is C3′-endo and the frequency of the associated guanine mode has recently been determined[41,42] to be 666 cm^{-1}. In rGMP, the extra hydroxyl group at the C2′-position increases the conformational flexibility of the sugar ring, and both C2′-endo and C3′-endo conformations are populated.[44] This inference is directly supported by the 218-nm-excited RR spectrum of rGMP, shown in Figure 5, which shows bands of nearly equal intensity at both 682 and 666 cm^{-1}, whereas the spectrum of dGMP shows a single band at 682 cm^{-1}, with only a shoulder at 666 cm^{-1} (suggesting some conformational flexibility even in this case). Another conformationally sensitive guanine mode was recently identified[16] at 855 cm^{-1} in dGMP. Figure 5 shows rGMP having an additional component of this mode at 864 cm^{-1}. This spectrum is better resolved and shows the 864/855-cm^{-1} bands more clearly than the one given in ref 16.

The middle spectrum of Figure 5 is that of the Ni–dGMP complex. Like rGMP, it shows components at 682/666 and 855/864 cm^{-1}, although the intensity distribution is somewhat different. The crystal structure[31b] of the Ni–dGMP complex (Figure 6a) shows the sugar having a C3′-endo conformation due to a bending back of the 5′-methylene group because of intramolecular H bonding from Ni-bound water molecules to the 5′-monophosphate group. The nonresonance Raman spectrum of this crystal[41] shows a guanine band at 666 cm^{-1}, as expected for the C3′-endo conformation. Thus the presence of both C3′-endo and C2′-endo bands in the solution UVRR spectrum indicates that the intramolecular H bonding to the phosphate group is maintained in only about half of the molecules in solution. In aqueous solution intermolecular H-bonding is available from the solvent water molecules. The UVRR spectrum suggests that the free energy is about the same for intra- and intermolecularly H-bonded phosphate; the intermolecularly H-bonded molecules revert to the C2′-endo sugar conformation.

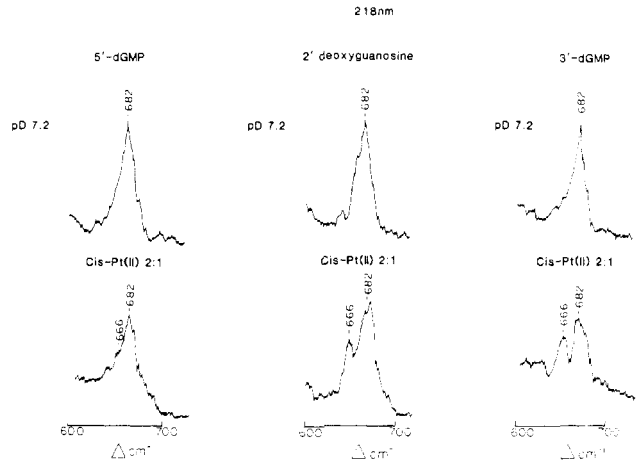

Figure 7. 600–700-cm^{-1} region of 218-nm-excited UVRR spectra of 5′-dGMP, 2′-deoxyguanosine, and 3′-dGMP (top) and of 2:1 complexes with *cis*-$(NH_3)_2Pt^{2+}$ (bottom), all in D_2O (used to aid in NMR characterization of the complexes).

Figure 7 shows that binding of *cis*-$(NH_3)_2Pt^{2+}$ also converts a fraction of the ribose rings to the C3′-endo conformation, but this phenomenon is *not* linked to an intramolecular H bond like the one found in the Ni–dGMP crystal structure. The 2:1 complex with 5′-dGMP shows a 666-cm^{-1} C3′-endo shoulder on the 682-cm^{-1} C2′-endo UVRR band, but the 666-cm^{-1} band is also pronounced for the 2:1 complex with 3′-dGMP, whose phosphate group is on the 3′-OH group of the ribose ring, a position less favorable to intramolecular H bonding. Moreover, a pronounced 666 cm^{-1} band is also seen for the 2:1 complex with 2′-deoxyguanosine, which lacks any phosphate group. (The 1:1 complexes of cis-$(NH_3)_2Pt^{2+}$ with 3′-dGMP and 2′-deoxyguanosine are unstable with respect to the 2:1 complexes.[22d] About half of the 666-cm^{-1} band intensity for the 3′-dGMP complex is attributable to a frequency shift of the 682-cm^{-1} band in the ~15–20% of the molecules that had undergone C(8) H/D exchange in the D_2O solution, as monitored by NMR. No exchange was detectable for the 5′-dGMP or 2′-deoxyguanosine complexes.)

NMR studies indicate a change from C2′-endo to C3′-endo conformation when the N7 of 5′-dGMP is protonated or methylated[46,47] or bound to $PtCl_3^-$.[47] In none of these cases can an intramolecular H bond be involved, and it has been suggested that the electrostatic interaction between the positively charged center at N7 and the phosphate group is sufficient to induce the conformation change. Our observation of a C3′-endo/C2′-endo mixture in the 2:1 complex of *cis*-$(NH_3)_2Pt^{2+}$ with 2′-deoxyguanosine, however, demonstrates that the phosphate group is not required for this effect in agreement with previous work.[46] On the other hand the Ni^{2+} complex of 2′-deoxyguanosine does not show a detectable 666-cm^{-1} band (spectrum not shown), indicating that for Ni^{2+} the interaction with phosphate, either electrostatic or via an intramolecular H bond, is required for C3′-endo stabilization. We tentatively infer that *cis*-$(NH_3)_2Pt^{2+}$, forming a stronger bond with N7, induces the ribose conformational change via an electronic polarization effect on the guanine ring. Methylation and protonation may have a similar effect.

(36) (a) Lord, R. C.; Thomas, G. J. *Spectrochim. Acta, Part A* **1967** *23A*, 2551. (b) Mansy, S.; Engstrom, S. K.; Peticolas, W. L. *Biochem. Biophys. Res. Commun.* **1975**, *68*, 1242. (c) Nishimura, Y.; Hirakawa, A. Y.; Tsuboi, M. *Adv. Infrared Raman Spectrosc.* **1978**, *5*, p 217.
(37) Pohl, F. M.; Ranade, A.; Stockburger, M. *Biochim. Biophys. Acta* **1973**, *335*, 85.
(38) Thamann, T. J.; Lord, R. C.; Wang, A. H. J.; Rich, A. *Nucleic Acids Res.* **1981**, *9*, 5443.
(39) Benevides, J. M.; Thomas, G. J., Jr. *Nucleic Acids Res.* **1983**, *11*, 5747.
(40) Chinsky, L.; Jolles, B.; Laigle, A.; Turpin, P. Y.; Taboury, J.; Taillandier, E. *Biopolymers* **1984**, *23*, 1931.
(41) Nishimura, Y.; Tsuboi, M.; Sato, T. *Nucleic Acids Res.* **1984**, *12*, 6901.
(42) Benevides, J. M.; Wang, A. H. J.; Rich, A.; Kyogoku, Y.; van der Marel, G. A.; van Boom, J. H.; Thomas, G. J., Jr. *Biochemistry* **1986**, *25*, 41–50.
(43) Tsuboi, M.; Takahasi, S.; Harada, I. In *Physico-chemical Properties of Nucleic Acids*; Duchesne, J., Ed.; Academic: New York, 1973; Vol. 2.
(44) Davies, D. B.; Danyluk, S. S. *Biochemistry* **1974**, *13*, 4417.
(45) Son, T. D.; Guschlbauer, W. *Nucleic Acid Res.* **1975**, *2*, 873–886.
(46) Kim, C. H.; Sarma, R. H. *J. Am. Chem. Soc.* **1978**, *100*, 1571–1590.
(47) Polissiuo, M.; Viet, M. T. P.; St.-Jacques, M.; Theophanides, T. *Can. J. Chem.* **1981**, *59*, 3297–3302.
(48) Kuntz, G. P. P.; Kotowycz, G. *Biochemistry*, **1975**, *14*, 4144.

Conclusions

The 218-nm-enhanced C=O6 stretching band of dGMP provides clear evidence for intramolecular H bonding to the O6 atom from metal-bound H_2O for N7-bound Ni^{2+} and *cis*-$(NH_3)_2Pt^{2+}$. When a second G is bound to the Pt, this interaction is abolished, and the C=O6 stretch increases in frequency due to polarization; a larger increase is seen when N7 is protonated. Polarization effects are also seen in frequency and/or intensity changes for several of the guanine ring modes. The sugar-conformation-sensitive guanine modes at 682/666 and 855/864 cm^{-1} indicate an equilibrium mixture of C2′-endo and C3′-endo conformations in the metal complexes, reflecting partial association of the 5′-monophosphate group with Ni^{2+}-bound H_2O molecules but a ring-polarization effect of bound *cis*-$(NH_3)_2Pt^{2+}$. These inferences about the details of the metal–dGMP structures in dilute aqueous solution illustrate the power of the UVRR technique in monitoring the chemical environment of nucleic acid bases.

Acknowledgment. We thank Professors Jan Reedijk and Luigi Marzilli for helpful discussions. This work was supported by NIH Grant GM 25158.

Contribution from the Department of Chemistry,
The University of Houston—University Park, Houston, Texas 77004

Electrochemistry of Iron Porphyrins under a CO Atmosphere. Interactions between CO and Pyridine

C. Swistak and K. M. Kadish*

Received August 19, 1986

The electrochemistry of (TPP)FeCl and (TPP)$FeClO_4$ were investigated in pyridine and in CH_2Cl_2 under a CO atmosphere. Five types of Fe(II) complexes and two types of Fe(I) complexes were spectrally and electrochemically identified. The Fe(II) complexes were (TPP)Fe, $[(TPP)FeCl]^-$, $[(TPP)Fe(CO)Cl]^-$, $(TPP)Fe(py)_2$, and (TPP)Fe(py)(CO) while the Fe(I) complexes were $[(TPP)Fe]^-$ and $[(TPP)Fe(CO)(py)]^-$. An overall oxidation/reduction scheme was formulated for the electrode reactions in pyridine and CH_2Cl_2 under a CO atmosphere. In addition, the kinetics for several ligand displacement reactions were investigated for complexes of Fe(III), Fe(II), and Fe(I) and formation constants for the addition of one or two CO molecules to $[(TPP)FeX]^-$ or (TPP)Fe in CH_2Cl_2 were calculated.

Introduction

The electrochemistry of synthetic iron porphyrins in pyridine and in pyridine/dichloromethane mixtures has been reported by a number of laboratories.[1,2] In the presence of pyridine, the Fe(III)/Fe(II) potentials of (P)FeX (where P is the porphyrin macrocycle and X is an anion other than ClO_4^-) are shifted positively from values obtained in noncomplexing media. At the same time potentials for the Fe(II)/Fe(I) reaction of (P)Fe are shifted negatively from those for reduction of the same complex in a nonbonding solvent. For example, values of $E_{1/2}$ for the first reduction of (TPP)FeX in CH_2Cl_2 (where TPP is the dianion of tetraphenylporphyrin) range between −0.19 V ($X = Br^-$) and 0.47 V vs. SCE ($X = F^-$). Under the same solution conditions, $E_{1/2}$ for the second reduction ranges between −1.06 and −1.07 V vs. SCE for (TPP)FeX complexes where $X = ClO_4^-$, Br^-, Cl^-, or N_3^-. The second reduction of (TPP)FeF is more difficult and occurs at −1.50 V vs. SCE in CH_2Cl_2, 0.1 M (TBA)ClO_4.[3] In contrast, the same porphyrins in pyridine containing 0.1 M (TBA)ClO_4 have $E_{1/2}$ values that range between 0.15 and 0.17 V (first reduction) and between −1.48 and 1.51 V (second reduction).[3] The invariant $E_{1/2}$ values are indicative of the fact that pyridine has replaced the counterion on Fe(III) so that the same six-coordinate $[(TPP)Fe(py)_2]^+$ species exists in solution.[1-3] Also, the increase in stabilization of iron(II) in pyridine (with respect to oxidation or reduction in CH_2Cl_2) is consistent with the fact that large binding constants are found for pyridine addition to (TPP)Fe(II) while much smaller interactions of pyridine occur with (TPP)FeX and no interaction occurs with $[(TPP)Fe^I]^-$.

Bis(pyridine) adducts are invariably formed with iron(II) porphyrins and values of $\beta_2 > 10^8$ have been calculated for (TPP)Fe in CH_2Cl_2 or benzene.[4,5]

$$(TPP)Fe + 2py \rightleftarrows (TPP)Fe(py)_2 \qquad (1)$$

Large binding constants may also be observed for complexation of pyridine by (P)FeX, but this will depend upon the nature of the anionic counterion, X^-, which will compete for the Fe(III) binding site. For example, values of $\beta_2 \approx 10^{7.5}$ are obtained for formation of $[(TPP)Fe(py)_2]^+X^-$ (reaction 2) when the metalloporphyrin is (TPP)$FeClO_4$.[5] On the other hand, much smaller binding constants are obtained when the porphyrin is (TPP)FeCl[6] or (TPP)FeF.[3]

$$(TPP)FeX + 2py \rightleftarrows [(TPP)Fe(py)_2]^+X^- \qquad (2)$$

Very little interaction occurs between the Fe(I) center of $[(TPP)Fe]^-$ and pyridine. It was long thought that nitrogenous bases and specificially pyridine could not bind to the iron(I) state of metalloporphyrins[1,2] but recent low-temperature ESR studies show this not to be the case.[7]

The above example of how pyridine binding affects iron porphyrin redox potentials is not limited to cases where the complexed ligand is a nitrogenous base. Similar examples of potential shifts upon ligand binding have been provided for iron(III) and iron(II) porphyrins containing bound sulfur donor ligands[8,9] as well as for complexation of the iron porphyrins with diatomic molecules such as NO, CS, CSe, O_2, or CO.[1,2] Substantial positive shifts of Fe(II) oxidation potentials also occur after complexation of a given synthetic iron(II) porphyrin with diatomic molecules such as NO, CS, and CSe, and for these later complexes the air-stable state of the porphyrin contains Fe(II).[10,11] This is in contrast to other

(1) See: Kadish, K. M. In *Iron Porphyrins, Part 2*; Lever, A. B. P., Gray, H. B., Eds.; Addison-Wesley: Reading, MA, 1983; pp 161–249.
(2) See: Kadish, K. M. *Prog. Inorg. Chem.* **1986**, *34*, 435–605.
(3) Bottomley, L. A.; Kadish, K. M. *Inorg. Chem.* **1981**, *20*, 1348.
(4) Brault, D.; Rougee, M. *Biochemistry* **1974**, *13*, 4591.
(5) Kadish, K. M.; Bottomley, L. A. *Inorg. Chem.* **1980**, *19*, 832.
(6) (a) Kadish, K. M.; Bottomley, L. A. *J. Am. Chem. Soc.* **1977**, *99*, 2380. (b) Satterlee, J. D.; La Mar, G. N.; Frye, J. S. *J. Am. Chem. Soc.* **1976**, *98*, 7275. (c) Walker, F. A.; Lo, M. W.; Ree, M. T. *J. Am. Chem. Soc.* **1976**, *98*, 5552.
(7) Srivatsa, G. S.; Sawyer, D. T.; Boldt, N. J.; Bocian, D. F. *Inorg. Chem.* **1985**, *24*, 2123.
(8) Wilson, G. S. *Bioelectrochem. Bioenerg.* **1974**, *1*, 172.
(9) Mashiko, T.; Marchon, J. C.; Musser, D. T.; Reed, C.; Kastner, M. E.; Scheidt, W. R. *J. Am. Chem. Soc.* **1979**, *101*, 365.

0020-1669/87/1326-0405$01.50/0